Arab J. Nucl. Sci. Appl., Vol. 55, 2, 1-8 (2022)

ISSN 1110-0451

Arab Journal of Nuclear Sciences and Applications

Web site: ajnsa.journals.ekb.eg

(E S N S A)

Analytical study of Radionuclide and Radon Concentrations in Rock Samples Collected from Um-Bogma and its Radiological Hazard Impact

S. M. Adel [1]*, T. M. Hegazy[1], T.M. Abd El Maksoud[1] and H. M. Diab[2].

[(1)] Physics Department, Faculty of women for Arts, science and Education, Ain Shams University, Cairo, Egypt.
[(2)] Nuclear and Radiation Safety ResearchCenter (NRSRC)Egyptian Atomic Energy Authority (EAEA), Egypt.

ARTICLE INFO

Article history:

Received: 12th July 2021

Accepted: 29th Dec. 2021

Keywords:

Radionuclides,
HPGe,
SSNTDs CR39,
Radon Concentrations,
Hazard Parameters.

ABSTRACT

The HPGe detector was used to calculate the specific activity of natural radionuclides 238U, 232Th, and 40K in rock samples obtained from the Um-Bogma area. Um-Bogma is divided into four regions: Abu Zarab, Sad Elbanat, TaletSelim, and Allouga. The dose rate and hazards parameters have been calculated. Concentration of ^{222}Rn emanated (^{226}Ra decaying) has been calculated using empirical formulae and compared with that measured using Solid State Nuclear Track Detector CR-39 (SSNTD). The average specific activity in Bqkg-1(dry weight) for 238U, 226Ra, 232Th and 40K were 396.3±3.3, 405.04±3.4, 61.45±1.3 and 377.2±5.8 , respectively for Abu Zarab area, 1216.6±5.4, 1475.4±6.7, 61.8±1.3 and 359.2±6.1 Bqkg-1 , respectively for Talet Seleim area, 467.8±4.2, 408.41±3.5, 29.60±0.9 and 259.2±2.9 Bqkg-1 , respectively for Allouga area and 557.05±4.1, 491.78±3.9, 63.45±1.4 and 420.55±3.6 Bqkg-1 respectively for Sad AlBanat area. The measured radon concentrations for the four regions were 4.95, 10.4, 4.6 and 3.9 Bq/m3. From the data obtained, it is found that the geological structure considered the main factor for the increase of radon concentration.

1-INTRODUCTION

The distribution of natural radionuclides and radiation levels in the environment are critical for determining the consequences of terrestrial radiation exposure. Soil naturally contains radionuclides such as 226Ra, 232Th, and 40K [1]. Because radionuclides in soil and rock are not equally dispersed, natural radioactivity is largely determined by rock formalizations and geographical circumstances, resulting in varying amounts of radionuclides in such media. [2] and [3] are examples of formalized paraphrases. Large quantities of materials containing naturally occurring radioactive elements are produced as a result of mining and other industrial operations (NORM) [4].

Natural radionuclides present may cause effects. The natural background radiation, which may consequently increase to significant levels, is of great concern to radiation protection regulatory bodies. ^{222}Rn is a daughter of ^{226}Ra and is in turn derived from the longer-lived antecedent ^{238}U. Inhalation of radon (^{222}Rn) may cause hazard lung effect [5, 6].

Um Bogma Formation located in south western Sinai, Egypt is considered as important region because it is rich with minerals such as uranium, Mn-Fe ore deposits and secondary copper mineralization [7].

This study aims to investigate the radionuclides and radon levels beside their hazard parameters in the Um-Bogma locality. High purity germanium (HPGe) detector was used to determine the specific activity concentration of radionuclides and radon concentration was determined by using Solid State Nuclear Track Detector (SSNTDs). Hazard parameters were estimated (radiation doses including the average radium equivalent (Raeq), total absorbed dose rate (D), external and internal hazard indices (Hex + Hin)) and effective dose due to external and internal exposure due to radon gas was also determined.

Corresponding author: shaimaaadelshosho@gmail.com
DOI: 10.21608/ajnsa.2021.85634.1485

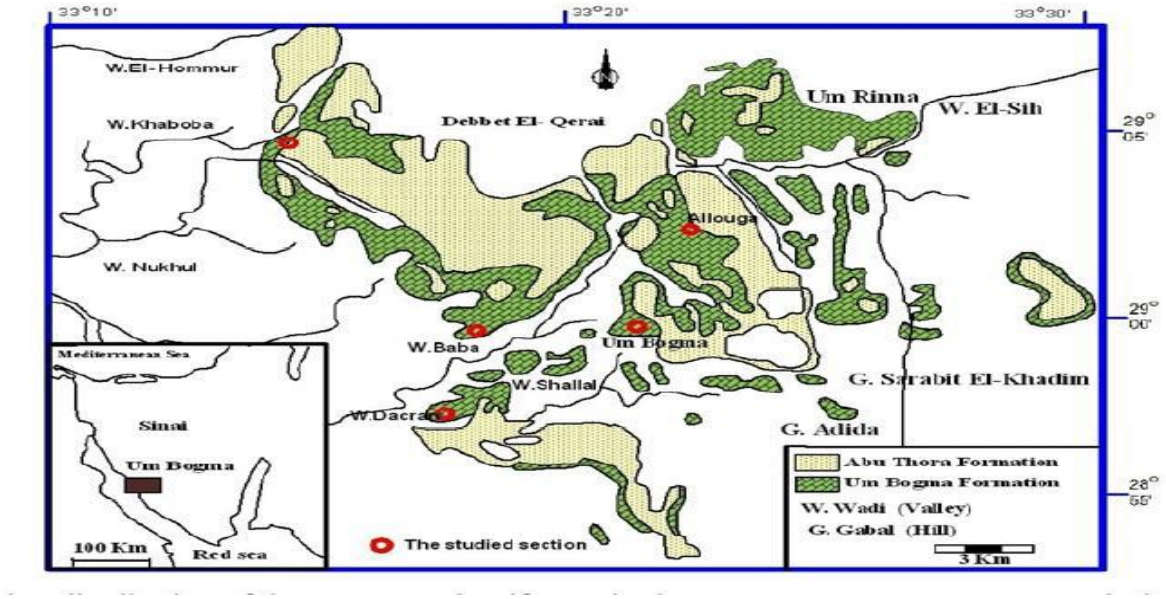

Fig. (1): Geologic map of the studied area

2-METHODOLGY

2.1. Site descriptions

The Um Bogma surroundings are located on the east shore of the Gulf of Suez, in southern Sinai, to the east of Abu Zeneima town. The area is about 700 km bounded by 33° 10`- 33° 32` E Longitudes and 28° 50`- 29° 05` N Latitudes as shown in figure. 1[8].

Many development initiatives are underway in South Western Sinai, including industrial zones, tourism activities, mining, habitation, and land reclamation. Um Bogma area considered as an important strategic site for some elemental production (U, Mn, Fe and Cu). The beneficial uses of the above mentioned minerals are very well known in different industrial domains. [9]. The samples were obtained from four major areas in Egypt's southwestern Sinai. Abu Zarab, Sad Elbanat, TaletSelim, and Allouga are the names of these areas .

2.2. Soil sample preparation

Twenty-two sedimentary rock samples were collected by random sampling method from the studied area. The samples were packed, labelled and transferred to the laboratory. Samples were dried in open air of a dry place, mechanically crushed, and sieved through a 2 mm mesh sieve then sealed in 100-ml capacity polyethylene Marinelli beakers and stored to reach secular equilibrium (prevent the escape of ^{222}Rn and ^{220}Rn) [10].

2.3. HP-Ge detector and γ-ray spectrometry

Non-destructive analysis was performed on the samples using a High-Purity Germanium HPGe detector. With a resolution of 1.9 keV and a peak/Compton ratio of 69.9:1 at the 1332 keV gamma-ray transition of 60Co, the detector has a relative efficiency of roughly 40% of the 3″ x 3″ Ge(Li) crystal efficiency. A 4 mm Pb, 1 mm Cd, and 1 mm Cu shield is employed to minimize background radiation. The gamma spectrometers were calibrated in the same geometry as the samples using both 226Ra point source and potassium chloride standard solutions. For the 226Ra (238U) series, the gamma transmissions used for activity estimates are 352.9 (214Pb), 609.3, 1120.3, and 1764.5 keV (214Bi), 338.4, 911.1, and 968.9 keV (228Ac) for the 232Th series, 1460.7 keV for 40K, 661.6 keV for 137Cs, and 46.5 keV for 210Pb [12]. A set of IAEA certified reference materials (IAEA-326, IAEA-375, IAEA-RGU, IAEA-CU-2008 and IAEA-152) were used for method verification. A period of 80,000s is adjusted for each sample and Genie 2000 software is used for gamma spectrum peak area analysis.

The specific activity (C) in units of Bqkg^{-1} is determined using the following equation [11]:

$$C(Bq\ Kg^{-1}) = \frac{C_n}{\varepsilon P_\gamma M_S} \qquad (1)$$

Where

C_n is the count rate under each photo-peak due to each radionuclide,

ε is the detector efficiency for the specific γ-ray,

P_γ is the intensity of the specific γ-ray, and

M_s is the mass of the sample (kg).

The lowest limits of detection (LLD) is determined using the following formula [13]

$$\mathbf{LLD} = \frac{4.66Sb}{\varepsilon \times I\gamma} \quad (2)$$

Where:

S_b is the estimated standard error of the net background count rate in the spectrum of the radionuclide.

I_γ is the intensity of the specific γ-ray.

The LLD values obtained were 2.15, 0.41 and 0.22 Bq kg^{-1} for ^{40}K, ^{238}Ra and ^{232}Th, respectively.

The average absorbed dose rate (nGy h−1) in air, 1 m above ground, was determined by [14]:

$$\mathbf{D(nGy/h) = 0.429\ A_{Ra} + 0.666\ A_{Th} + 0.042\ A_K} \quad (3)$$

where A_U, A_{Th} and A_K are the activity concentrations of ^{226}Ra, ^{232}Th and ^{40}K, respectively.

The annual effective dose was computed as follow:

$$\mathbf{OEDR\ (mSv/y) = D \times 24h\ d^{-1} \times 365.25d\ y^{-1} \times 0.6\ (OCPF) \times 0.7\ SvGy^{-1}\ (CONVC) \times 10^{-6}} \quad (4)$$

Where

OEDRis the outdoor effective dose rate (in mSv y^{-1})

OCPF and CONVC are the occupancy factor and conversion coefficient, respectively,

D is absorbed dose rate (nGy h−1) .

Because the indoor and outdoor occupancy factors must add up to 1.0 in order to account for 100% of the group's exposure time, we calculated the indoor effective dose rate (IEDR in mSv y1) is calculated as follows:

$$\mathbf{IEDR = D \times 24\ h\ d^{-1} \times 365.25\ d\ y^{-1} \times 0.4\ (OCPF) \times 0.7\ Sv\ Gy^{-1}\ (CONVC) \times 10^{-6}} \quad (5)$$

The radium equivalent activity is a weighted sum of activities of 226Ra, 232Th and 40K based on the presumption that 10Bqkg-1 of 226Ra, 7Bqkg-1 of 232Th or 130Bqkg-1 of 40K produce the same gamma- ray dose rates. Hence it is defined as follows:

$$\mathbf{Ra_{eq} = A_{Ra} + 1.43\ A_{Th} + 0.77A_K} \quad (6)$$

where A_{Ra}, A_{Th}, and A_K are the activity of 226Ra, 232Th, and 40K in Bqkg-1, respectively. For an external dosage of 1.0 mGy/y, Raeq must be 370 Bqkg-1.[15]

The external hazard index Hex is a modified amount of radium equivalent activity that is defined as follows::

$$\mathbf{H_{ex}} = \frac{\mathbf{A_{Ra}}}{\mathbf{370}} + \frac{\mathbf{A_{Th}}}{\mathbf{259}} + \frac{\mathbf{A_K}}{\mathbf{4810}} \quad (7)$$

To maintain the radiation danger relevant, the value of Hex must be less than one [16]. Equation (8) was used to calculate the excess lifetime cancer risk factor (ELCR).

$$\mathbf{ELCR = AED \times DL \times RF} \quad (8)$$

Where DL and RF are the duration of life (70 years) and risk factor 0.05 Sv-1, respectively

2.4. Solid State Nuclear Track Detector (SSNTD) CR-39:

SSNTD is one of the most important tools for radon measurements [17] . It is sensitive to heavy particles. CR-39 sheets of 25cm x 30cm and a thickness of 1mm were cut into small detector of size 1 cm × 1 cm. It was prepared and placed in the chamber cover's bottom. For 30 days, the compartment was sealed and kept. During that period, the CR-39 captured the tracks of alpha particles caused by the decay of radon and its daughters that had entered the chamber's air volume. The CR-39 detectors were etched in 6.25 N NaOH at 70°C for 6 hours after exposure, and the track density was measured using an optical microscope.

2.5. Radon Concentration Measurement:

The engraved traces on the detectors were manually numbered by examining pictures captured with an optical microscope at 400 times magnification. A stage eyepiece was used to compute the area of one field of vision, and the track density was estimated in terms of tracks per cm^2; the background track density was determined by etching a virgin detector under the identical circumstances. The measured track density was removed from the backdrop.

To get accurate statistics on the tracks, 20 fields of view on the detector surface were chosen at random. The calibration factor of 0.18 0.002 tracks cm^2 obtained from a previous calibration experiment for the (CR-39) track detector [18] was used to calculate radon activity from track density using the equation given by [19]:

$$\mathbf{C_{Rn} = (N - B) / t\ C_F} \quad (9)$$

where C_{Rn} is the mean Rn-222 concentration in Bqm-3, N is the track density (Track.cm-2), B is the background track density (Track.cm-2), C_F is the calibration factor (cm-2 d-1 per Bqm-3) and t is the exposure duration (hours).

Concentration of ^{222}Rn emanated from samples as a result of ^{226}Ra decaying has been calculated from measured radium activity concentrations using UNSCEAR empirical formulae with the following construction [20]:

$$A_R = C_R \cdot \rho \cdot A_{Ra} \quad (10)$$

Where:

A_R is concentration of radon gas emanated from collected sample (Bq/m^3).

C_R is the emission constant of ^{222}Rn from collected sample, which is equal to o.1.

ρ is the sample bulk density in (Kg/m^3) .

A_{Ra} is ^{226}Ra activity concentrations present in peatmoss sample (Bq/Kg)

3. RESULTS AND DISCUSSIONS

3.1. Gamma- ray counting:

The specific activity of ^{238}U, ^{226}Ra, ^{232}Th and ^{40}K are listed in Table (1). As shown in figure (2), Talet Seleim Region recorded the maximum radiation level.

The specific activity for ^{238}U (Bq/kg) ranged from 84.2 ± 1.7to 2596.3± 10 with an average 607.1 ± 5.9, 226Ra (Bq/kg) from 15.3±0.4 to 3384.5±12 with an average 647.8±4.2 , 232Th (Bq/kg) ranged from 7.6±0.2 to 128.4±2.1 with an average 56.65±1.24. Finally, the obtained results for 40K (Bq/kg) ranged from 15.1±0.4 to 818.1±11.8 with an average 348.12 ±5.7

The factors affecting uranium distribution in Um Bogma Formation, southwest Sinai are related mainly to the physical properties of the rocks and the subsequent geochemical processes affecting these rocks. The diagenetic processes are very important in improving the physical properties of the carbonate rocks for minerals deposition. Dissolution is one of the isochemical processes which result in stylolites and secondary porosity. Most of the channel porosity was filled with Mn-Fe oxides which have its role in the uranium distribution. The compaction led to the formation of some which represent pathways for uranium solutions. Cementation of the calstic rocks below the carbonate rocks and the presence of siltstone and claystone make barrier which trapped the uranium solutions to form the peneconcordant uranium mineralization

Table (1): Distribution of activity concentrations for different radionuclides in (Bq kg^{-1}) measured by gamma counting

Sample	^{238}U seies		Th-^{232}	K-^{40}
	Pa-^{234}	Ra-^{226}		
A1	**536.1±3.1**	651.6±3.6		
A2	**133.9±1.7**	164.6±1.9	55.8±1.2	180.5±3.5
A3	**761.3±4.8**	1007.2±6.1	108.2±1.9	645.5±8
A4	**428.8±3.5**	206.1±2.5	99.2±1.8	341.8±5.4
A5	**154.8±1.8**	120.1±1.8	18.8±0.6	157.8±3.6
A6	**346.3±3.7**	386.7±3.8	68.3±1.5	438.6±6.6
A7	**182.4±2.3**	144.02±2.1	70.9±1.6	199.2±4.3
A8	**84.2±1.7**	15.3±0.4	7.6±0.3	15.1±0.4
A9	**306.6±3.5**	314.9±3.3	99.5±1.8	631.3±7.7
A10	**110.1±1.8**	112.8±1.9	14.1±0.6	200.8±4.3
A11	**285.1±3.9**	230.3±3.7	69.9±2	818.1±11.8
A12	**1426.3±8.8**	1506.6±9.2	77.3±1.8	607±8.6
Average	**396.3**±3.3	405.04±3.4	61.45±1.4	377.20±5.8
T1	**1344.9±4.6**	1688.9±6.5	41.7±1.1	151.8±3.7
T2	**312.1±3.2**	182.4±2.9	50.7±1.4	574.8±9.2
T3	**2596.3±10**	3384.5±12	128.4±2.1	531.8±7.2
T4	**316.1±3.3**	185.2±2.4	24.8±0.7	303.1±5.3
T5	**1513.9±6.3**	1741.9±9.1	32.3±1.1	242.7±5.5
Average	1216.6±5.4	1475.43±6.6	61.83±1.3	359.20±6.1
G1	**478.8±4.1**	260.3±2.7	30.1±0.8	156.3±3.4
G2	**653.4±6.2**	520.4±5.1	17.9±0.8	234.6±5.6
G3	**271.1±2.5**	444.5±3.7	40.8±1.1	386.7±5.7
Average	**467.7**±4.2	408.41±3.5	29.60±0.9	259.2±2.9
S1	**395.3**±3.1	260.9±3.2	67.3±1.5	447.9±7.1
S2	**718.8±5.1**	722.7±5.2	59.6±1.6	393.2±7.5
Average	557.05±4.1	491.78±3.9	63.45±1.4	420.55±3.6

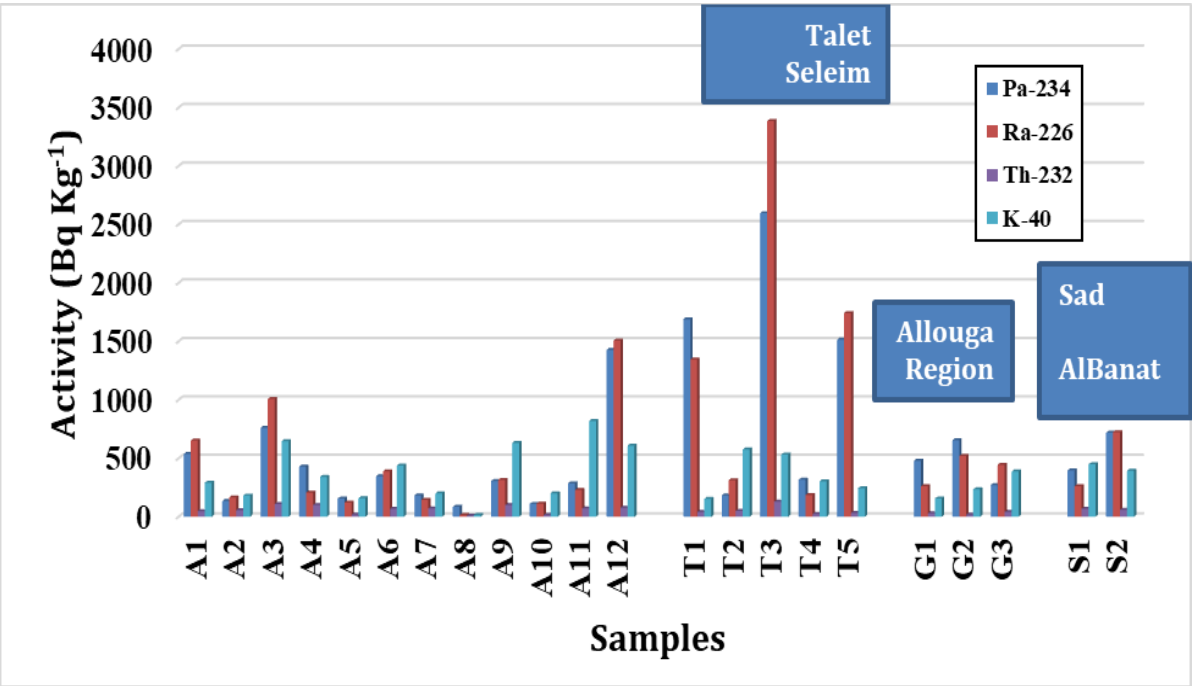

Fig. (2): Distribution of activity concentrations for different radionuclides in (Bq kg^{-1})

Figure (3): represents the ^{226}Ra - ^{238}U activity relation, good correlation has been found between ^{238}U and its daughter ^{226}Ra, which a positive correlation between U-^{238} and Ra-^{226} due to secular equilibrium between them reflect the nature of studied locality with equilibrium characteristics. Figure (4) represents the ^{40}k – ^{232}Th relation, no correlation has been found between ^{40}k – ^{232}Th.

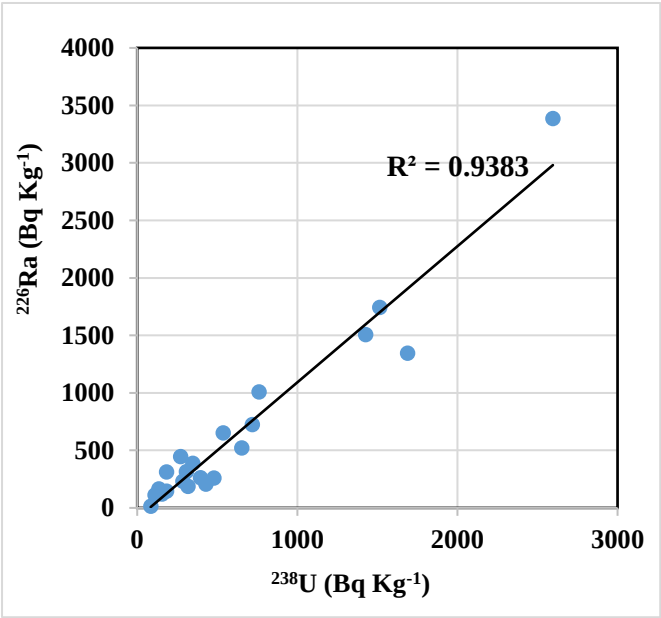

Fig. (3): Activity concentrations of ^{226}Ra vs ^{238}U for different samples

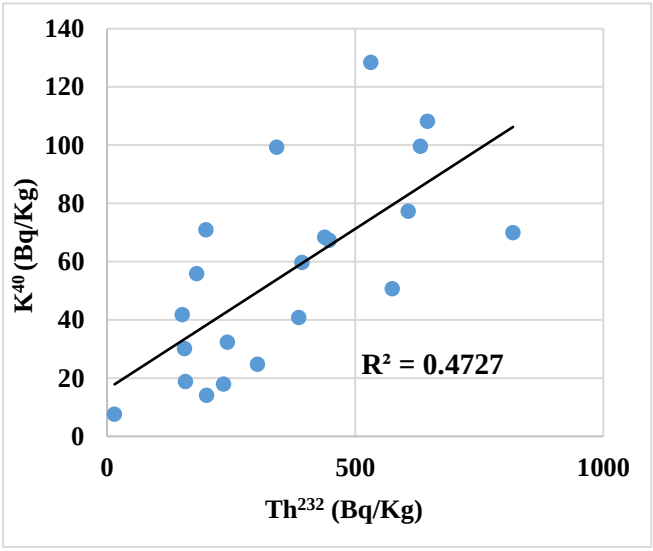

Fig. (4): Activity concentrations of 40 K vs 232Th for different samples

Internal hazard index, and excess lifetime cancer risk, respectively was calculated by the gamma spectrometric techniques and are listed in table (2). The lowest value for the external hazard index was 0.14 and the highest value was 19.9 with an average value namely 4.43. The lowest value for the internal hazard index was 0.07 and the highest value was 9.75 with an average value namely, 2.03 and the calculated values of excess lifetime cancer risk (ELCR)for the studied samples are higher than the unity (except for A8 sample).

Table (2): Hazard's parameters of the investigated samples

Sample	H_{in}	H_{ex}	ELCR
A1	1.7	3.52	7.37
A2	0.70	1.48	2.90
A3	3.27	7.20	13.70
A4	1.01	2.21	4.20
A5	0.43	1.05	1.80
A6	1.40	3.27	5.90
A7	0.70	1.47	2.90
A8	0.07	0.14	0.30
A9	1.37	3.40	5.70
A10	0.40	1.08	1.70
A11	1.06	3.22	4.50
A12	4.50	9.70	18.80
T1	4.76	9.61	19.90
T2	0.81	2.38	3.40
T3	9.75	19.90	40.80
T4	0.66	1.73	2.80
T5	4.88	10.04	20.40
G1	0.85	1.85	3.60
G2	1.52	3.37	6.40
G3	1.44	3.36	6.04
S1	1.06	2.60	4.40
S2	2.27	4.95	9.50
AVERAGE	2.03	4.43	8.50

Absorbed dose rates and annual effective dose rates (indoor and outdoor) for the samples under investigation were calculated and are listed in table (3). The dose rate range from (12.42 n Gy/h) to (1665.56 n Gy/h) with an average (347.20n Gy/h), since the world exposure dose rate was (70 n Gy/h), we find that the average dose rate is larger than the world average dose rate. The minimum, the maximum and the average values for outdoor annual effective dose rate are 0.02 mSv/y, 2.04 mSv/y and 0.43 mSv/y, respectively and the corresponding indoor annual effective dose rate values are 0.06 mSv/y, 8.17 mSv/y and 1.70 mSv/y, respectively. This result points to a dangerous effect in that region for human health. Therefore, suitable precautions and safety rules should be strictly applied for any industrial activity.

Table (3): Dose rate (nGy/h), indoor and outdoor annual effective dose rate (mSv/y)

Sample	Dose rate	AEDR (indoor)	AEDR (outdoor)
A1	301.10	1.48	0.37
A2	118.20	0.58	0.15
A3	559.40	2.74	0.69
A4	171.10	0.84	0.21
A5	73.70	0.36	0.09
A6	239.40	1.17	0.29
A7	118.90	0.58	0.15
A8	12.42	0.06	0.02
A9	233.60	1.15	0.29
A10	69.30	0.34	0.08
A11	183.90	0.90	0.23
A12	769.40	3.77	0.94
T1	812.50	3.99	1.00
T2	139.70	0.69	0.17
T3	1665.56	8.17	2.04
T4	113.60	0.56	0.14
T5	834.90	4.10	1.02
G1	145.50	0.71	0.18
G2	261.30	1.28	0.32
G3	246.80	1.21	0.30
S1	180.90	0.89	0.22
S2	387.30	1.90	0.48
AVERAGE	347.20	1.70	0.43

3.2 Radon concentration:

Radon concentration from CR39 recorded tracks has been calculated using equation. (9) and compared with expected emanated radon by using equation.(10) according to radium activity measured by gamma counting for different studied samples and displayed in figure (5) and table (4).

Table (4): Experimental and Calculated of Radon Concentration (Bq/Kg)

Sample	RnC $_{exp}$	RnC $_{cal}$
A1	22.90	37.87
A2	5.48	6.32
A3	10.92	18.09
A4	2.86	4.89
A5	1.89	2.89
A6	3.82	6.74
A7	1.42	2.70
A8	0.48	0.56
A9	3.67	6.17
A10	1.83	2.75
A11	1.77	3.83
A12	2.39	7.67
T1	7.16	13.55
T2	1.44	1.68
T3	24.07	40.33
T4	2.87	6.46
T5	16.42	24.43
G1	4.07	9.50
G2	5.30	6.53
G3	4.53	10.82
S1	2.57	4.90
S2	5.29	5.98

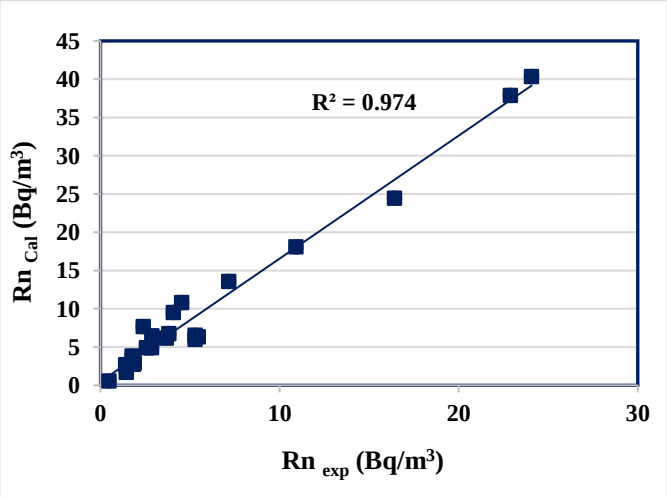

Fig. (5): Correlation between Experimental and Calculated of Radon Concentration for different samples

The Total effective dose from gamma and radon for all the studied samples, for different corresponding regions, are listed in Table (5).

Table (5): Total effective dose from gamma and radon (mSv/y)

Sample	D(radon)	D(gamma)	total effective dose
A1	0.393848	1.846075	2.239923
A2	0.094175	0.725086	0.819261
A3	0.187846	3.430461	3.618308
A4	0.049131	1.049143	1.098275
A5	0.032489	0.452181	0.48467
A6	0.065721	1.468056	1.533777
A7	0.02434	0.72897	0.75331
A8	0.008228	0.076146	0.084375
A9	0.063146	1.432577	1.495723
A10	0.03156	0.42469	0.45625
A11	0.030419	1.128082	1.15850
A12	0.041169	4.717743	4.758911
T1	0.123134	4.982495	5.105629
T2	0.024844	0.856805	0.88165
T3	0.413968	10.21321	10.62718
T4	0.04937	0.696305	0.745675
T5	0.28242	5.119652	5.402072
G1	0.070074	0.891962	0.962036
G2	0.091096	1.602475	1.693572
G3	0.077957	1.51353	1.591487
S1	0.044141	1.109841	1.153983
S2	0.09099	2.375111	2.466101

4-CONCLUSIONS:

This study was concerned with the investigation of the activity concentration of ^{238}U, ^{226}Ra, ^{232}Th and ^{40}K using HPGe detector and estimation of hazard parameters due to radioactivity levels for each selected sample. The radon concentration level was measured using SSNTDs .The determination of the effective dose due to external and internal radon was also calculated .From the data obtained, it is concluded that more safety precautions must be taken due to the geological formation of the area under study.

5-REFERENCES:

[1] Yadav, M., Rawat, M., Dangwal, A., Prasad, M., Gusain, G.S. and. Ramola, R.C. (2014) Levels and Effects of Natural Radionuclides in Soil Samples of Garhwal Himalaya, *J Radioanal Nucl Chem* ,**302** (2), 869–873.

[2] Gregory, A.O. (2005) Determination of Radionuclide Level in Soil and Water around Cement Companies in Port Harcourt. *Journal of Applied Sciences and Environment Managemental(JASEM),* **9** (3) , 27–29.

[3] UNSCEAR (2000) REPORT Vol.1 Sources and Effects of Ionizing Radiation.United Nations Scientific Committee on the Effect of Atomic Radiation. UNSCEAR (2000) Report to the General Assembly annexes, United Nations, New York. USA.

[4] Samuel, O.F., Kayode, O.O. and Bamidele, O.H. (2011) Radiological Indices of Technologically Enhanced Naturally Occurring Radionuclides: A PIXE approach, J. *Radiol Prot.*,**31**(2), 255–264.

[5] Al-Jarallah, M., ur-Rehman, F., Musazay, M.S. and Aksoy, A. (2005) Correlation between Radon Exhalation and Radium Content in Granite Samples Used as Construction Material in Saudi Arabia, *Radiat. Meas* ,**40**(2), 625–629.

[6] UNSCEAR (2008) REPORT Vol.1 Sources and Effects of Ionizing Radiation. United Nations Scientific Committee on the Effect of Atomic Radiation. UNSCEAR (2000) Report to the General Assembly annexes, United Nations, New York. USA.

[7] Abbas, A.E.A. (2020) Geology and Mineralogy of the Radioactive Ferruginous Siltstones at Wadi El Seih Area, Southwestern Sinai, Egypt, *IOSR Journal of Applied Geology and Geophysics*, **8**(3) Ser. I, 29-42.

[8] Ramadan, F.S. (2014) Petrographic and Diagenetic Characteristics of the Dolomites at Um Bogma Formation (Early Carboniferous), West Central Sinai, Egypt. *World Appl. Sci. J.*,**31**(1), 12-30.

[9] El-Kameesy, S. U., Abd El-Gowad, N. M. and Diab, H. M (2017) Natural Radioactivity and Environmental Impact in Um Bogma, South Western Sinai, Egypt, *Arab Journal of Nuclear Sciences and Applications (AJNSA)* ,**50**(4), 48-54.

[10] Veiga, M.M. and Baker R.F. (2004). Global Mercury Project. Protocols for Environmental and Health Assessment of Mercury Released by Artisanal and Small Scale Gold Miners. Vienna: GEF/UNDP/UNIDO.

[11] Jibiri, N.N., Farai, I.P. and Alausa, S.K. (2007) Estimation of Annual Effective Dose Due to Natural Radioactive Elements in Ingestion of Foodstuffs in Tin Mining Area of Jos-Plateau, Nigeria. *J. Environ. Radiat.,* **94** (1), 31–40.

[12] Technical Reports Series, (1989). Technical Reports Series No.295, Measurement of Radionuclides in Food and the Environment, A Guidebook, IAEA, Vienna-Austria.

[13] Jibiri, N.N. and Bankole, O.S. (2006) Soil Radioactivity and Radiation Absorbed Dose Rates at Roadsides in High-Traffic Density Areas in Ibadan Metropolis, southwestern Nigeria. *Radiat. Prot. Dosimetry*, **118**(4), 453–458.

[14] OECD, Organization for Economic Cooperation and Development, (1979): Exposure to Radiation from Natural Radioactivity in Building Materials. Report by a Group of Experts of the OECD Nuclear Energy Agency, OECD, Paris.

[15] Huy, N.Q. and Luyen, T.V. (2006) Study on External Exposure Doses from Terrestrial Radioactivity in Southern Vietnam. *Radiat. Prot. Dosimetry* , **118**(3),331-336 .

[16] Hilal, M.A. and Borai, E.H. (2018) Hazardous Parameters Associated with Natural Radioactivity Exposure from Black Sand. *Regul. Toxicol. and Pharmacol.*, **92**, 245–250.

[17] Durrani, S.A. and Bull, R. K. (1987). Solid State Nuclear Track Detection: Principles, Methods and Applications, 1st Edition, Pergamon Press, Oxford, UK.

[18] Khan, A.J., Varshney, A.K., Parsed, R., Tyagi, R.K. and Ramachandran, T.V. (1990) Calibration of (CR-39) Plastic Track Detector for the Measurement of Radon and its Daughters in Dwellings. *Nucl Tracks Radiat Measure* ,**17**, 497–502.

[19] Tanner, A.B. (1980). Radon Migration in the Ground: A Supplementary Review. Proceedings of Natural Radiation Environment III: Springfield, US DOE Report Number CONF-780422, 1, Reference Number 12618303.

[20] UNSCEAR (1988). Sources, Effects and Risks of Ionizing Radiation. United Nations Scientific Committee on the Effect of Atomic Radiation. UNSCEAR 1988 Report to the General Assembly, with Annexes. United Nations, New York. USA.